Shim, B. O., Chung, S. Y., Kim, H. J., Sung, I. H., IRF-k kriging of electrical resistivity data for estimating the extent of saltwater intrusion in a coastal aquifer system. International Symposium on the Fusion Technology of Geosystem Engineering, Rock Engineering and Geophysical Exploration
Seoul, Korea, Nov. 18-19, 2003

IRF-k kriging of electrical resistivity data for estimating the extent of saltwater intrusion in a coastal aquifer system

B. O. Shim[1], S. Y. Chung[2], H. J. Kim[2], I. H. Sung[1]

[1]Korea Institute of Geoscience and Mineral Resources, Daejeon, Korea, [2]Pukyong National University, Busan, Korea

Abstract: We have evaluated the extent of saltwater intrusion from electrical resistivity distribution in a coastal aquifer system in the southeastern part of Busan, Korea. This aquifer system is divided into four layers according to the hydrogeologic characteristics and the horizontal extent of intruded saltwater is determined at each layer through the geostatistical interpretation of electrical resistivity data. In order to define the statistical structure of electrical resistivity data, variogram analysis is carried out to obtain best generalized covariance models. IRF-*k* (intrinsic random function of order *k*) kriging is performed with covariance models to produce the plane of spatial mean resistivities. The kriged estimates are evaluated by cross validation to show a good agreement with the true values and the statistics of cross validation represented low errors for the estimates. In the resistivity contour maps more than 5 m below the surface, we can see a dominant direction of saltwater intrusion beginning from the east side. The area of saltwater intrusion increases with depth. The northeast side has low resistivities less than 5 ohm-m due to the presence of saline water in the depth range of 20 m through 70 m. These results show that the application of geostatistical technique to electrical resistivity data is useful for assessing saltwater intrusion in a coastal aquifer system.
Keywords: coastal aquifer, cross validation, electrical resistivity, geostatistics, IRF-*k* kriging, saltwater intrusion

1. Introduction

Well monitoring and vertical electrical sounding (VES) are used to define a contaminated area by saltwater intrusion in a coastal aquifer in Busan, Korea. The VES method is widely used and applied to the evaluation of aquifer contamination [e.g., *Stewart et al.*, 1983; *Ebraheem et al.*, 1990; *Zhody et al.*, 1974]. It is one of the most economical methods for surveying seawater intrusion but the interpretation is difficult according to the subsurface condition. The electrical resistivity of rock depends on lithology and fluid content. The resistivity of identical porous rock samples varies considerably with the salinity of saturated water. The higher the salinity of pore water, the lower the resistivity of rock. As a result, the number and thicknesses of geoelectrical units determined from VES measurements may not be necessarily same with the geological ones at a locality. The resistivity significantly varies with small changes in water salinity, and this property is very suitable for groundwater exploration with low cost [*Sabet,* 1975]. Electrical resistivities at a VES station or electrical conductivities (EC) in a monitoring well permit the estimation of saltwater concentration only at the location where resistivity or EC measurements are done. So spatially denser measurements may be necessary to define accurate range or concentration of intruded saltwater. To this end a geostatistical approach is demanded to generate reliable unbiased spatial data using the limited number of data. Application of geostatistical techniques to geophysical data is discussed by *Parks and Bently* [1996], *Cassiani and Medina* [1997], *Kalinski et al.* [1993], and *Troisi et al.* [2000].

In the procedure to estimate spatial data, the selection of geostatistical methods is important. When the spatial statistical structure of data shows a trend, the intrinsic random function of order *k* (IRF-*k*) can be useful to make spatial prediction of variables with a trend component [*Cressie*, 1993]. The idea is to use higher order differences to filter out polynomials of degrees 1, 2,..., *n*. The function for such differences is called the generalized covariance (GC) of order *k*. The use of IRF-*k* kriging is an established practice for the estimation of spatial variable for geological properties. As a best linear unbiased estimator the kriging technique is applied to electrical resistivity data to produce best estimates with fitted GC models. The estimates are examined with cross validation tests and the scatter diagrams of original values versus estimates are analyzed.

This study is aimed for providing a useful methodology to define the extent of intruded saltwater with widely used geophysical technique applying geostatistical method. We interpret VES curves and calculate spatial mean resistivities of specified layers. The kriged contour maps of resistivity distribution can be used to represent the horizontal extent of intruded saltwater in each layer.

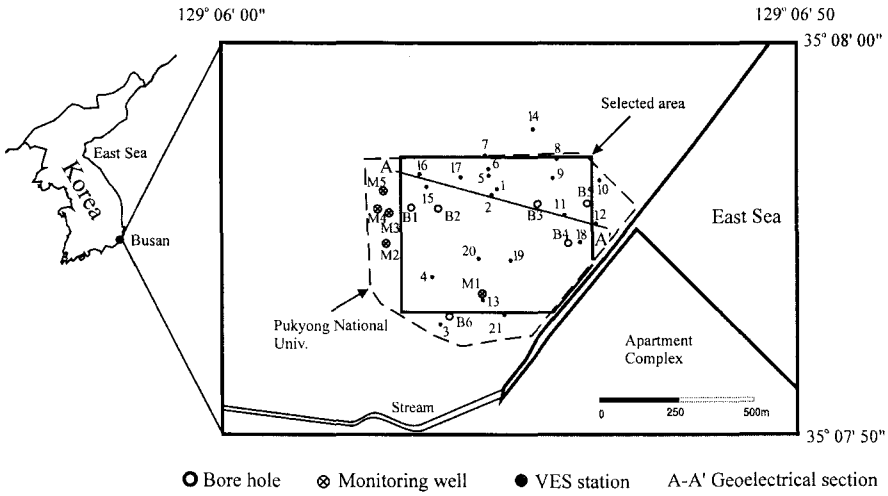

Figure 1. Location map of study site showing boreholes, monitoring wells, VES stations, and a geoelectrical line.

2. Hydrogeological settings

Figure 1 shows a location map of this study site and a small area (600 m by 500 m) is selected for geostatistical analysis of VES data. The eastern boundary of the selected area is contacted with a long narrow path filled with seawater. The annual rainfall of Busan during 1993 - 2002 ranged from 960 mm to 2002 mm and the major portion (rainfall) occurred during summer. Freshwater derived from the rainfall seeps through the shallow porous strata and reserves to the fractured rock aquifer, which is composed of andesitic volcanic breccia and tuffaceous sediment rock complex. In the alluvium and volcanic rock aquifer, recharged ground water forces saltwater out and makes a hydrostatic balance with intruded saltwater in the transition zone. Ground water is unconfined in shallow aquifer consisted with alluvium and weathered soil zone. While ground water in fractured rock aquifer deeper than 20 m b.g.l. (below ground level) is confined.

The general direction of ground water flow is eastward, which is deduced from the feature of topography and watershed of this study site. The relief of the selected area is very low and the average elevation is about 5 m above the mean sea level. There are five monitoring wells: well M1 is located at 180 m from the southeastern boundary, and the other boreholes are installed near the west boundary (Figure 1). The mean hydraulic gradient of ground water is in the range of 0.006 – 0.008. *Shim et al.* [2002] derived a relationship between TDS and EC as TDS (mg/l) = 0.70 × EC_{25} (μS/cm) from 39 water samples in the monitoring wells. EC logging is performed in the monitoring well M1 having 120 m deep (Figure 2). The EC range is from 1618 to 26,850 μS/cm, and the value is rapidly increased from 25 m deep and marks 26,850 μS/cm in 35 m deep. The rapid increase is caused by the hydrodynamic characteristics of the transition zone between freshwater and saltwater. The fluctuation of EC below 30 m b.g.l. represents the heterogeneity of aquifer system generating vertically different hydrostatic balance between freshwater and saltwater. EC shows an inverse relationship with distance from the coastline as shown in Table 1. The high EC value in well M1 is rapidly decreased to the range of 595 – 1081 μS/cm in wells M2, M3, M4 and M5.

Table 1. Distance from the coastline, well depth, EC and sampling depth in monitoring wells.

Monitoring well	Distance from coastline (m)	Well depth (m)	EC (μS/cm)	Sampling depth (m)
M1	180	120.0	22,610	50
M2	516	35.0	1081	33
M3	612	50.4	838	46
M4	634	40.2	664	39
M5	660	43.1	595	40

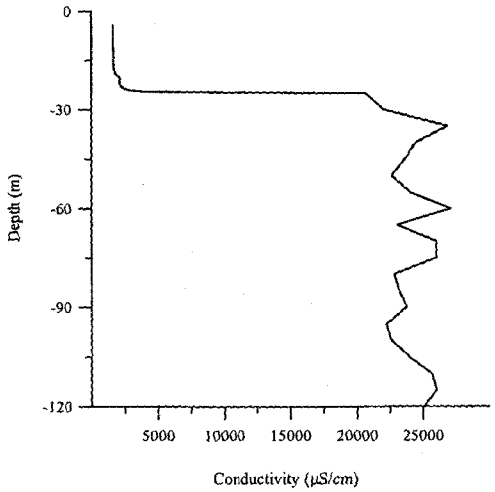

Figure 2. Electrical conductivity log measured in monitoring well M1.

This aquifer system can be divided vertically to four horizontal hydrogeologic units (layers) according to different sedimentary and hydrogeological characteristics: The surface layer up to 5 m deep is characterized by several deposits, which are consisted with highly permeable landfill materials including grabble, coarse sand, and medium sand. The thickness of this layer is slightly increased in the east side and the water table is in the range of 3 – 5 m b.g.l. The second layer of 5 – 20 m is saturated and mainly composed of weathered soil consisting of silty sand, sandy clay and find sand. The third layer of 20 – 40 m, which is consisted of weathered soft rocks, is highly fractured and contains thin clay layer less than 10 cm thickness, confirmed in a few boreholes in the west side. Slug tests shows the hydraulic conductivity of this unit ranges from 5.93×10^{-8} to 5.02×10^{-6} m/s. The lower boundary of this zone includes weathered rock and highly fractured softrock. The final, fourth layer of 40 – 70 m is consisted of fractured soft rocks, and the hydraulic conductivity is lower than those of the above units. To compromise the interpreted description of each sounding curve with the divided hydrogeologic units, lower boundary of this range is constrained to 70 m b.g.l. because the spacing between current electrodes is limited to 200 m. The hydrogeology of 70 – 120 m deep showed similar state with the above layer in well M1.

3. Geophysical surveys

Twenty one VESs employing a Schlumberger electrode configuration were conducted in May, 2000. We used a resistivity sounding unit, the Syscal Model manufactured by IRIS instruments, and current electrode spacings (AB/2) are ranged from 1.5 m to 100 m. VES lines are unified to the east-west direction because the transition zone has the south-north direction. The objective of these electrical soundings is to deduce the variation of electrical resistivities with depth and to correlate these with geological knowledge for inferring the subsurface structure in greater detail [*Zohdy et al.*, 1974]. Within a given rock type, the resistivity of rock varies primarily due to the quality and quantity of water contained in the rock and the presence of clay. Therefore, higher clay content and/or poorer quality (higher TDS and/or chlorides) ground water lowers the rock resistivity. In the four hydrogeological units described in the last section, thin clay layer is found at the second unit and only a few boreholes on the west side contain clay in the upper boundary of the third unit.

VES curves are interpreted and compared with EC data collected in the monitoring wells (Figure 3). As an inverse modeling program, *RESIX*^{plus} [1992] has been used to get geoelectrical layer parameters from a fitted model. The number of geoelectrical layers is interpreted as 3 or 4, and the first and second geoelectrical layers show generally small thicknesses (less than 10 m). The average resistivities of the first two geoelectrical layers are about 80 and 60 ohm-m respectively. A few VES stations positioned near the coastline show very low resistivity (less than 2.0 ohm-m) at the last geoelectrical layer, which may be saturated with saline water (10,000 – 100,000 mg/l TDS). In order to bring out the horizontal extent of the saline water intrusion, interpreted resistivity data from the 21 soundings are utilized for the preparation of mean resistivity contour maps of the four horizontal slices with 0 – 5, 5 – 20, 20 – 40 and 40 – 70 m depth ranges. The mean resistivity ρ_m is defined by

$$\rho_m = \frac{1}{z_2 - z_1} \int_{z_1}^{z_2} \rho(z) dz, \tag{1}$$

where z_1 and z_2 represent the depths of lower and upper boundaries of a subsurface layer, respectively, and $\rho(z)$ indicates the resistivity at depth z.

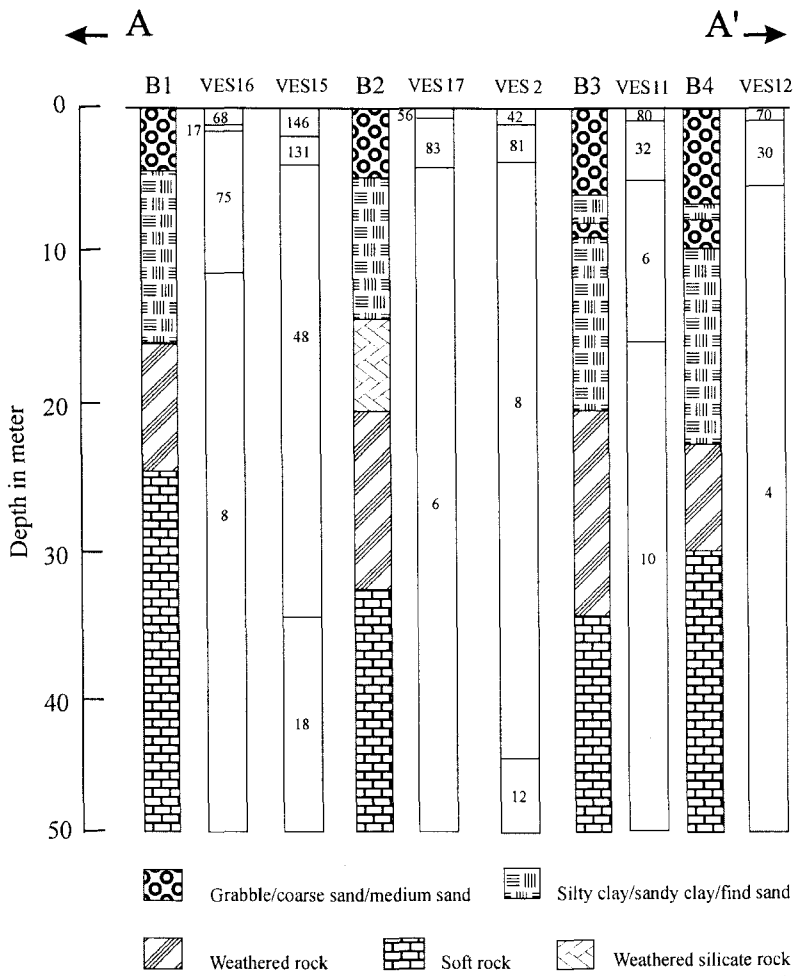

Figure 3. Layered model interpretation of VES data with borehole logging data along line A-A'.

4. IRF-*k* kriging theory

The theory of IRF-*k* was formulated by *Matheron* [1973] and refined later by *Delfiner* [1976]. On a domain let us consider a random function (RF) $Z(x)$, where x is the co-ordinate of the domain. The function $Z(x)$ can be decomposed into two components: a deterministic component $m(x)$, the drift, and a fluctuation random function $Y(x)$ having zero mean:

$$Z(x) = m(x) + Y(x), \tag{2}$$

$$E[Z(x)] = m(x). \tag{3}$$

The drift $m(x)$ can be modeled as a polynomial, by a linear combination of deterministic elementary monomials with exponent $l = 0, \ldots, k, f_l(x) = x^l$:

$$m(x) = \sum_{l=0}^{k} a_l f_l(x), \tag{4}$$

where the coefficients a_l cannot be all zero. For $k = 0, f_0(x) = 1$ and $m(x) = a_0$, then the drift is a constant and from the point of view RF can also be stationary. For $k \geq 1$ RF is nonstationary.

This method uses generalized covariance instead of typical variogram models as

$$K_k(h) = C\delta(h) + \sum_{j=0}^{k} \alpha_j \mid h \mid^{2j+1}, \tag{5}$$

where $\delta(h)$ is the Dirac delta function, C is the covariance, h is the separation distance of data fair, and α_j is the coefficient of GC model.

Neither the order of IRF nor the generalized covariance of field data is known in advance. The following parameter estimation procedure is performed with the AKRIP code developed by *Kafritas and Bras* [1981] using an iterative regression approach based on the *Delfiner*'s algorithm for the determination of polynomial GC: (1) determination of order k, (2) estimation of the coefficients of polynomial GC, and (3) kriging of data with the determined GC. The constraints of the coefficients are $\alpha_0 \leq 0$, $\alpha_2 \leq 0$, $\alpha_1 \geq -\sqrt{10}\sqrt{\alpha_0\alpha_2}$ (for 3-D), and $\alpha_1 \geq -\frac{10}{3}\sqrt{\alpha_0\alpha_2}$ (for 2-D). The coefficients of GC are determined from the application of the weighted least-squares method to sample data [*Delfiner*, 1976].

5. Variogram analysis

The analysis of variogram is a very crucial part in geostatistical method and represents the spatial structure of data. Variogram of mean resistivities in each layer shows weak stationarity and represents some trends as shown in Figure 4 We use an IRF-k in the presence of trends with unknown parameters to analyze the spatial structure of data.

The jackknife method is used to select the best parameters for a GC model of polynomial. The jackknife is known very effective to estimate confidence limits for an unknown parameter whose population distribution cannot be assumed to be normal, and has proved to be a robust and powerful statistical tool [*William*, 1987]. In the procedure to select the parameters of GC model, the calculated jackknife estimator should be approximately 1.0. The order k is identified to be zero for the first layer and one for the other layers. Only the variogram of the first layer shows a stationary drift but those of other units represent nonstationarity. The GC models are determined by *Delfiner's* [1976] ranking comparisons. Each selected GC model indicates a satisfying result in the jackknife validation, because the calculated jackknife estimator is close to 1.0 (Table 2).

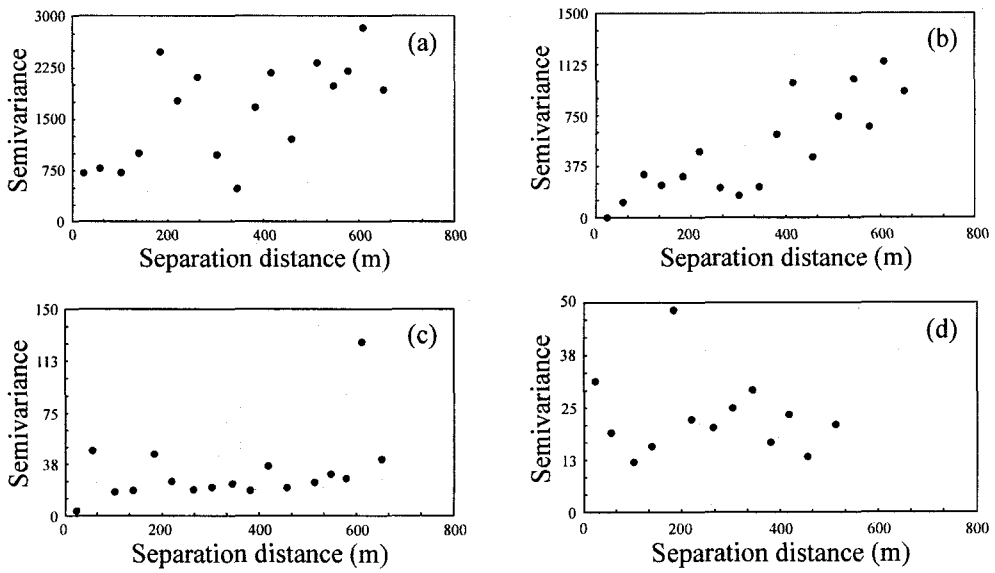

Figure 4. Variograms of VES data for four hydrogeological units of 0 – 5 (a), 5 – 20 (b), 20 – 40 (c), and 40 – 70 m (d) deep.

Table 2. Identified IRF orders, selected generalized covariance models, and jackknife estimators for each layer.

Depth (m)	k order	GC model	Jackknife
0 – 5	0	GC = -24.627 h	0.986
5 – 20	1	GC = 0.921	0.921
20 – 40	1	GC = 72.099	0.988
40 – 70	1	GC = 15.448 + 5.650×10^{-5} h^3	1.077

6. Cross validation

The closeness of predicted values to true values can be characterized in various ways. We use cross validation to verify the accuracy of estimated electrical resistivities. Table 3 represents the results of cross validation tests using the above statistical equations [Appendix]. In the 0 – 5 m depth MKV is very close to VE, and SDRE is very close to 1.0, but SRMSE, MSE, and MKV are higher than those of the other depth ranges. MRSE, SDRE and VRE of the first layer are similar to those of the other layers, but the other statistics are higher than those of the other layers.

Actually, if a satisfying fit of theoretical model to data was found, a graph of true values versus estimated values should result in a straight line with a slope of 1.0 [*Horn*, 1999]. Each plot of Figure 5 shows a similar agreement between true and estimated values, and the cloud of points indeed lies along the line with the slope of 1.0 in each scatter plot. Figure 5a presents a more or less circular cloud shape, while Figures 5b and 5d show some linear shape of clouds along a line with the slope of 1.0. In contrast, Figure 5c show the least relationship between the cloud of points and the line of slope of 1, and the estimates have higher values of MRSE, SDRE, VE, and VRE than those of the other layers (Table 3). We can find a similar shaped error in low resistivity data of each layer and the cause of the error is mainly due to the interpretation method of VES curves, which are obtained near coastline.
Hence the most of the estimates are shown reasonable.

Table 3. The results of cross validation tests to examine the accuracy of estimates generated by IRF-k kriging.

Statistics	0 – 5 m	5 – 20 m	20 – 40 m	40 – 70 m
ME	0.967E + 00	0.353E + 01	0.102E + 01	0.811E - 02
MSE	0.223E + 04	0.210E + 03	0.886E + 02	0.248E + 02
SRMSE	0.472E + 02	0.145E + 02	0.941E + 01	0.498E + 01
MKV	0.223E + 04	0.478E + 02	0.197E + 02	0.827E + 01
MRE	0.144E - 01	0.749E + 00	0.347E + 00	0.301E - 01
MSRE	0.103E + 01	0.196E + 01	0.209E + 01	0.203E + 01
VE	0.234E + 04	0.208E + 03	0.922E + 02	0.261E + 02
VRE	0.111E + 01	0.345E + 01	0.449E + 01	0.434E + 01
SDRE	0.105E + 01	0.186E + 01	0.212E + 01	0.208E + 01

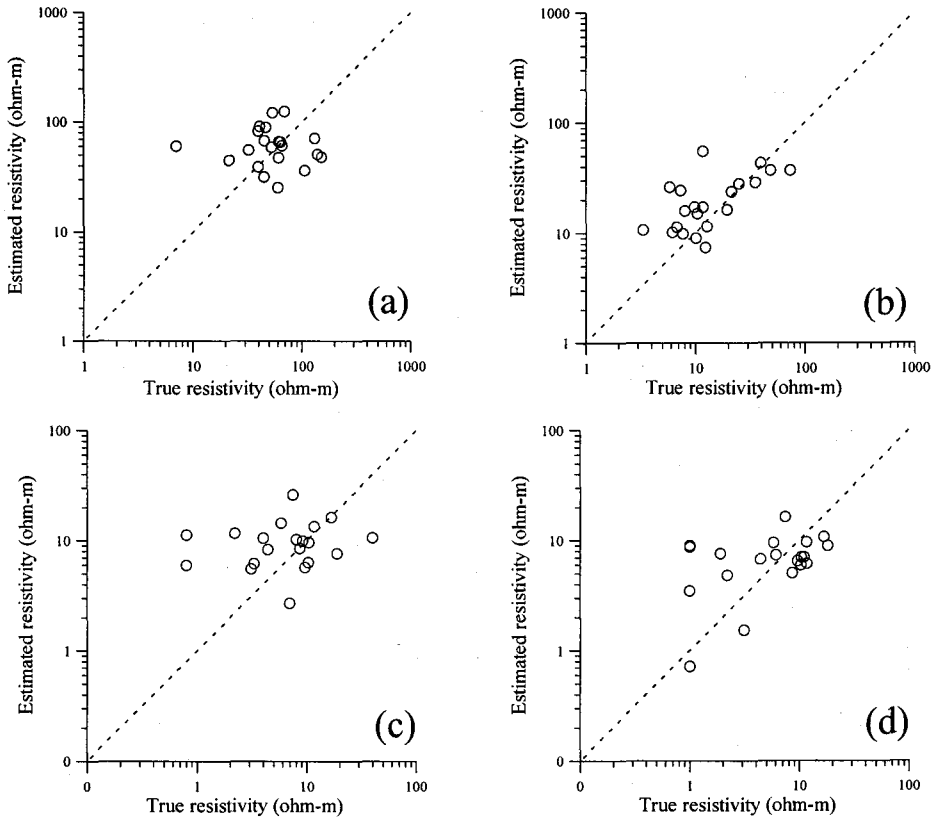

Figure 5. Graphical validation of estimates with original electrical resistivities for the depth ranges of 0 – 5 (a), 5 – 20 (b), 20 – 40 (c), and 40 – 70 m (d).

7. Extent of saltwater intrusion

The IRF-*k* kriged resistivity data are interpreted and evaluated to delineate the extents of saltwater intrusion in the each layer. In order to correlate the mean resistivity distribution with the concentration of intruded saltwater, we are required to know the minimum resistivity in the freshwater area in the aquifer system. Ground water having TDS as less than 1000 mg/l is considered to be in the quality of fresh water [*Freeze and Cherry*, 1979]. By comparing the estimated layer resistivity and EC in the monitoring wells, we determined the minimum resistivity for freshwater area as 15 ohm-m.

Figure 6a shows the contour map of the 0 – 5 m depth layer representing higher mean resistivity distribution than those of the other layers. The western part shows slightly higher resistivity distribution than the eastern or southeastern side, but it is uncertain to deduce the effect of saltwater intrusion from the contour map. The other contour maps (Figures 6b, 6c, and 6d) show a dominant direction of saltwater intrusion originated from the eastern side, and have low resistivity contour lines less than 15 ohm-m in the east side. The major part of the northeast side shows low resistivity distribution less than 15 ohm-m in Figure 6b. Around wells M2, M3, M4, and M5 the resistivity range is 55 – 60 ohm-m, while 25 – 30 ohm-m near well M1. Figure 6c shows that the electrical resistivity ranges from 4 to 22 ohm-m in the third layer, and the contour lines in the west area are arrayed in the north-south direction. The electrical resistivity near the monitoring well M1 is 8 ohm-m or less, which may represent the presence of saline water. Figure 6d is covered with the resistivity contours less than 15 ohm-m in the whole area. The low resistivity less than 5 ohm-m in the northeastern area represents the saline water intrusion, and the southeastern boundary shows slightly higher resistivity in Figures 6c and 6d.

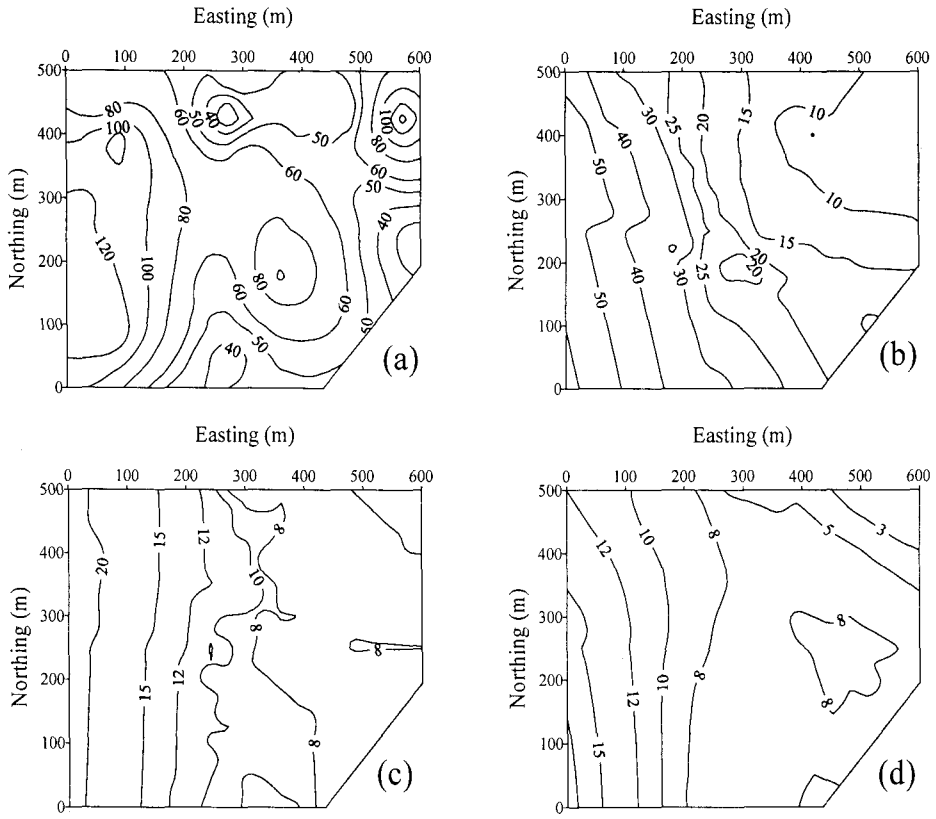

Figure 6. IRF-k kriged contour maps of electrical resistivity distribution for layers of 0 – 5 (a), 5 – 20 (b), 20 – 40 (c), and 40 – 70 m (d) deep. Contour values are in ohm-m.

Figure 7 shows the apparent resistivity section along line A-A'. Most area below 40 m deep is marked by contour lines less than 20 ohm-m except near the western boundary. The apparent resistivity distribution of the eastern boundary is less than 5 ohm-m, but that of the western boundary is in the range of 40 – 50 m ohm-m below 40 m deep. The low resistivity can be interpreted as a contaminated area due to saltwater intrusion. However, higher resistivity distribution between the western boundary and the position (center) of VES 17 can be regarded as an evidence of reduced saltwater concentration. The apparent resistivity distribution at the eastern boundary is less than 5 ohm-m, but that of the western boundary is in the range of 40 – 50 ohm-m below 40 m deep in the section. From this illustration, we can estimate the direction of saltwater intrusion, which is come from the eastern boundary

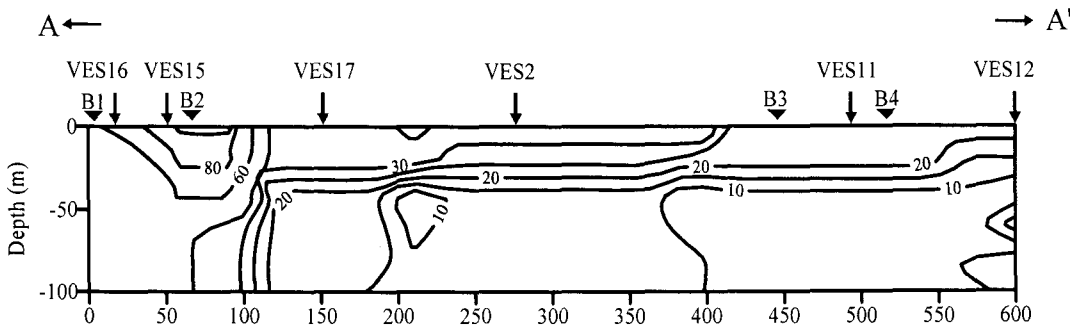

Figure 7. Isopleths map of apparent resistivity section along line A-A'. Kriged contour values are in ohm-m. The symbols ▼ and ↓ above the section represents the position of borehole and VES station, respectively.

8. Conclusions

The geostatistical method has wide applicability in areas where saltwater intrusion is certain in a coastal groundwater system and in areas where groundwater is highly contaminated with other originated saltwater in inland. However, owing to the lack of data having deeper information, the vertical extents of transition zone have high uncertainty and are not readily definable. This study showed that even though the available data were insufficient the horizontal extent of saltwater intrusion in a coastal aquifer system can be expected with a special use of geostatistical method.

We have applied the IRF-k kriging technique to the estimation of spatial data of electrical resistivity measured in the campus of Pukyong National University, and examined the estimates by cross validation. The determined k order and GC models produce reliable spatial data in the estimation of resistivity. In the hydrogeologic units of 5 – 20, 20 – 40, and 40 – 70 m deep the resistivity contour maps represent a dominant direction of saltwater intrusion beginning from the east boundary. However the direction is not clear in the layer of 0 – 5 m deep. The boundary of saltwater intrusion is delineated with the contour line of 15 ohm-m in the horizontal resistivity distribution of each layer. The extent of intruded saltwater varies with layer and the area occupied by saltwater is extended with depth. Only the east half of the area is occupied by saltwater in the layer of 5 – 20 m deep, while most of the area is contaminated in the layer of 40 – 70 m deep.

Appendix. Cross validation

The procedure of cross validation is as follows: First, values are estimated at known points with kriging as if the known points were unknown; one sample point is left out of the data set and a value is estimated at that location by kriging with a selected variogram model and the remaining data [*Davis*, 1987]. Next the errors of estimate are calculated from the true values. A reduced error (RE) is defined by the error divided by the square root of kriging variance of an estimate:

$$RE = \frac{Z(x) - Z^*(x)}{\sqrt{\sigma_K^2}}, \tag{A1}$$

where Z is the true value, Z^* the estimated value by kriging, and σ^2_K the kriging variance. If a selected model is the most suitable, the mean of reduced errors (MRE) should be close to zero and the standard deviation of reduced errors (SDRE) should be close to 1.0 [*Davis*, 1987; *Solow*, 1990]:

$$MRE = \frac{1}{N}\sum_{i=1}^{N}\left[\frac{Z(x) - Z^*(x)}{\sqrt{\sigma_K^2}}\right]_i \approx 0, \tag{A2}$$

$$VRE = \frac{1}{N-1}\sum_{i=1}^{N}(RE - MRE)_i^2, \tag{A3}$$

and

$$SDRE = \sqrt{VRE} \approx 1.0. \tag{A4}$$

In addition, some other statistics are also useful to the selection of the best model. The mean error (ME) should be close to zero, and the mean square error (MSE), the square root of mean square error (SRMSE) and the mean kriging variance (MKV) should be minimal. *Samper* [1986] also suggested that the variance of errors (VE) should be equal to the mean kriging variance (MKV).

$$ME = \frac{1}{N}\sum_{i=1}^{N}[Z(x) - Z^*(x)]_i, \tag{A5}$$

$$MSE = \frac{1}{N}\sum_{i=1}^{N}[Z(x) - Z^*(x)]^2{}_i, \tag{A6}$$

$$SRMSE = \sqrt{MRE}, \tag{A7}$$

$$MKV = \frac{1}{N}\sum_{i=1}^{N}(\sigma_K^2)_i\,, \tag{A8}$$

and

$$VE = \frac{1}{N-1}\sum_{i=1}^{N}(ERROR - ME)_i^2 = MKV \tag{A9}$$

where Error = $Z(x)$ - $Z^*(x)$.

Acknowledgments

This project was supported through the cooperative research project of the Korea Institute of Geosciences and Mineral Resources and Pukyong National University, No. 03-3211.

References

Cassiani, G., and M. A. Medina Jr., 1997, Incorporating auxiliary geophysical data into ground-water flow parameter estimation, *Ground Water*, *35*, 79-91.

Chung, S. Y., D.H. Kang, H.Y. Park, and B.O. Shim, 2000, Application of geostatistical methods for the analysis of groundwater contamination in Busan (Korea), *J. Korean Soc. Eng. Geol.*, *10*, 247-261.

Cressie, N. A. C., 1993, *Statistics for Spatial Data*, John Wiley & Sons, Inc.

Davis, B. M., 1987, Uses and Abuses of Cross-Validation in Geostatistics, *Math. Geol.*, *19*, 241-248.

Delfiner, P., 1976, Linear Estimation of Non Stationary Spatial Phenomena, *Advanced Geostatistics in the Mining Industry*, edited by M. Guarascio, M. David, and C. Huijbregts, D. Reidel Pub., Dordrech-Holland, 49-68.

Ebraheem, A. M., M. W. Hamburger, E.R. Bayless, and N.C. Krothe, 1990, A study of acid mine drainage using earth resistivity measurements, *Ground Water*, *28*, 361-368.

Freeze, R. A. and J. A. Cherry, 1979, *Groundwater*, Prentice-Hall.

Kafritas, J., and R. L. Bras, 1981, The practice of kriging, Ralph M. Parsons and Laboratory, Dept. of Civil Engineering, MIT Technical Report No. 263.

Kalinski, R. J., W. E. Kelly, and I. Bogardi, 1993, Combined use of geoelectrical sounding and profiling to quantify aquifer protection properties, *Ground Water*, *31*, 538-544.

Horn, M. E., 1999, *Geostatistics and Petroleum Geology*, Kluwer academic Pub.

Matheron, G., 1973, The intrinsic random functions and their applications, *Advanced Applied Probability*, *5*, 439-468.

Parks, K. P., and L. R. Bentley, 1996, Enhancing data worth of EM survey in site assessment by cokriging, *Ground Water*, *34*, 597-604.

RESIX ^{plus}, 1992, User's Manual, Interpex, Golden, USA.

Sabet, M. A., 1975, Vertical Electrical Resistivity Soundings To Locate Ground Water Resources: A Feasibility Study, VPI-WRRC-BULL 73, Virginia Polytechnic Institute and State University.

Samper, F. J., 1986, Statistical Methods of Analyzing Hydrological, Hydrochemical, and Isotopic Data from Aquifers, Ph.D. Dissertation, Dept. of Hydrology and Water Resources, University of Arizona, Tucsan.

Shim, B. O., S. Y. Chung, H. J. Kim, I. H. Sung, and B.W. Kim, 2002, Characteristics of sea water intrusion using geostatistical analysis of geophysical surveys at the southeastern coastal are of Busan, Korea, *J. Korean Soc. Soil and Groundwater Environment*, *7*, 3-17.

Shim, B. O., 2003, Characteristics of Hydrodynamic Seawater intrusion at the Southeastern Coastal Area of Busan (Korea), Ph.D. thesis, Pukyong Univ., Korea.

Solow, A. R., 1990, Geostatistical Cross-Validation: A Cautionary Note, *Math. Geol.*, *22*, 637-639.

Stewart, M., M. Layton, and T. Lizanec, 1983, Application of resistivity survey to regional hydrogeologic reconnaissance, *Ground Water*, *21*, 42-48.

Troisi, S., C. Fallico, S. Straface, and E. Migliari, 2000, Application of kriging with external drift to estimate hydraulic conductivity from electrical-resistivity data in unconsolidated deposits near Montalto Uffugo, Italy, *Hydrogeol. J.*, *8*, 356-367.

William, B. S., 1987, *Use and Abuse of Statistical Methods in the Earth Sciences*, Oxford Univ. Press.

Zhody, A. A. R., G. P. Eaton, and D. R. Mabey, 1974, Application of surface geophysics to ground water investigations. Techniques of Water-Resources Investigations of the U.S. Geological Survey, Chapter D1, Book2.